G. Almandoz, S. Zarate, A. Egea, Y. Moreno, A. Urdangarin and R. Moreno, "High Frequency Modeling of Electric Drives for Electromagnetic Compatibility Analysis," *2020 International Conference on Electrical Machines (ICEM)*, Gothenburg, Sweden, 2020, pp. 1129-1135.

DOI: https://doi.org/10.1109/ICEM49940.2020.9270804

High Frequency Modeling of Electric Drives for Electromagnetic Compatibility Analysis

G. Almandoz, *Member, IEEE*, S. Zarate, A. Egea, Y. Moreno, A. Urdangarin and R. Moreno

***Abstract*—In the present paper a time domain simulation of the overall electric drive, comprising the power converter, the power cables and the electrical machine is developed in order to analyse in detail the electromagnetic compatibility of the system. The simulations are validated by experimental test performed over an industrial converter-motor system, and a very good agreement is obtained between the simulation results and the experimental measurements.**

***Index Terms*—Electric Machines, Permanent magnet machines, Computer simulation, Electromagnetic compatibility**

I. Introduction

Variable Speed drives are supplied by Voltage Source Converters (VSC). Based on the modulation principle, the VSC can fed the motors by voltages with variable amplitude and frequency. Under this operation mode, high frequency harmonics are created, which could compromise the Electromagnetic Compatibility (EMC) of the overall drive system. In order to work it out, different solutions such as active filters [1] or special converter topologies [2], [3] are found to be technically suitable. Using this kind of solutions, both conducted currents and radiated noise can be notably reduced, so that the electric drive could comply with the EMC directives. Nevertheless, these solutions might increase the cost of the overall electric drive leading to less competitive devices. Thus, the high frequency behaviour of all elements comprising the electric drive must be more and more optimized in order to avoid any kind of problems related to the Electromagnetic Interferences (EMI), and in order to enhance the competitiveness of the electric drive.

The electric machine is the main element of a electric drive system. Generally electric machines are designed to fulfil some main design requirements such as torque density, torque ripple, energy consumption or noise and vibrations. Nevertheless, typically the EMC is not included among these design specifications [4]. Doing it perhaps the overall system could be optimized as the filter size could be probably reduced, leading to more cost-effective solutions. For that purpose, it is very important to develop fast simulation models that enables to analyse accurately the high frequency behaviour of the overall electric drive.

Concerning the high frequency model of electrical machines, many publications can be found in the literature. The most extended modelling techniques are based on lumped parameter models [5]–[17]. Common mode (CM) and differential mode (DM) impedances are measured in the frequency range between 150 kHz and 30 MHz. After that, model parameters are adjusted using experimentally measured impedance curves. Generally, the proposed models are validated experimentally with different degree of accuracy and detail. For instance, in [11], [16] only the motor model is validated analysing the CM currents in the time domain [11], or the CM voltages in the frequency domain [16]. Whereas in [5], [7] the overvoltages at motor terminal due to the effect of the cables are studied. In [6], [9] the effect of the cable length is analysed as well, but in this case only CM currents are analysed, and only time domain simulation results are compared with experimental measurements. In [12] the time domain CM voltages and currents are evaluated either, in simulation and experimentally, considering both, the motor model and the cable model. The EMC of an electric drive depends mainly on the voltage harmonics created by the power converter. However, in the aforementioned references, the converter is not included in the analysis.

Probably the most detailed studies are presented in [5], [13] as the overall drive system comprising the inverter, the cable and the motor is simulated and validated experimentally. In these papers CM voltages and currents are validated in the time domain, by experimental measurements, achieving to some extent good agreements. Nevertheless, the CM voltages and currents are not analysed in the frequency domain, in the complete range between 150 kHz and 30 MHz, in which the electric drives must comply with the EMC directives.

In the present paper a time domain simulation for the overall electric drive system comprising the power converter, the power cable and the PMSM is carried out. First, high frequency models for each element are developed. Second, the overall system is simulated obtaining CM voltages and currents. Finally, experimental tests are performed over an industrial electric drive and the simulations are validated comparing the CM voltage and current spectrums in the complete range of 150 kHz - 30 MHz. As a result, fairly good agreements between the spectrums estimated in simulation and the spectrums measured experimentally are reported.

G. Almandoz, S. Zarate, A. Egea and Y. Moreno are with the Informatic and Electronic Department of Mondragon Unibertsitatea, Mondragon, 20500, Gipuzkoa, Spain (e-mail: galmandoz@mondragon.edu, szarate@mondragon.edu, aegea@mondragon.edu, yerai.moreno@alumni.mondragon.edu,).

A. Urdangarin is with ORONA EIC, Hernani, 20120, Gipuzkoa, Spain (e-mail: aurdangarin@orona-group.com)

R. Moreno is with IKERLAN, Arrasate, 20500, Gipuzkoa, Spain (e-mail: rmoreno@ikerlan.es)

II. Description of the High Frequency Models

In this chapter the high frequency models for the three main elements comprising the electric drive, the electrical machine, the power cables and the inverter, are described. These models have been adjusted for an industrial electric drive consisting of a permanent magnet (PM) Brushless AC motor, by experimental tests. The obtained results by the proposed models are compared with the experimental measurements. This way it is validated that the proposed models represent properly the high frequency behaviour of every analysed element.

A. High Frequency Model for the PMSM

The adopted universal equivalent circuit for the PMSM is shown in the Fig. 1 [5], [12]. This circuit consisting of several concentrated parameters such as resistances, inductances and capacitances, takes into account different physical phenomena that arise in high frequency operation. R_{g1}, C_{g1} are the phase to ground equivalent resistance and parasitic capacitance, whereas R_{g2}, C_{g2} are the neutral to ground equivalent resistance and parasitic capacitance. R_e accounts for the high frequency magnetic losses, R_{cu}, L_d represent the winding resistance and inductance, and R_t, L_t, C_t are included to consider the stator inter-turn effect.

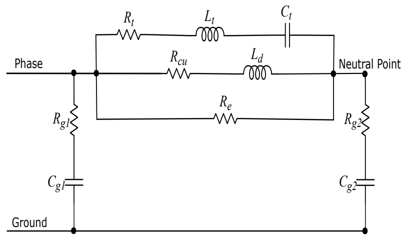

Fig. 1. Single phase high frequency model for the PMSM

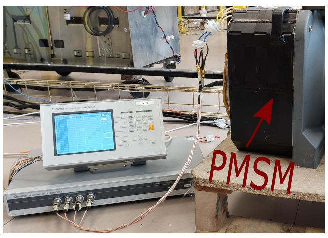

Fig. 2. Layout for the experimental measurement of the CM and DM impedances of the PMSM using the LCR meter

In order to adjust the parameters of the equivalent circuit, the CM and the DM impedances are measured in the frequency bandwidth 100 Hz - 30 MHz, using the LCR meter, model 11050-30M of CHROMA (see Fig. 2). Using these curves, the values of the parameters of the equivalent circuit are adjusted applying the procedure described in [7] (see results in the Table I) .

In the Fig. 3 the measured CM and DM impedances are plotted. In addition, the estimated curves using the proposed

TABLE I
Calculated values for the parameters of the electrical equivalent circuit of the PMSM

Parameter	Value	Parameter	Value
R_{g1}	27,74 Ω	R_t	11,64 KΩ
C_{g1}	196,72 pF	C_t	260,57 pF
R_{g2}	631,26 Ω	L_t	6 mH
C_{g2}	1,37 nF	R_{cu}	1,50 Ω
R_e	6,67 Ω	L_{cu}	5,3 mH

model are compared in the same graphic. As the studied frequency range is limited to 150 kHz - 30 MHz, the model is adjusted in this bandwidth. Due to that, the DM impedance is not properly represented in the frequency band below 150 kHz. Moreover, the are some high frequency effects in the range of 10-30 MHz which can not be thoroughly represented by the proposed model. Probably, implementing a more complex model with more parameters the very high frequency behaviour could be somehow improved [7], [11]. Nevertheless, this would complicate the model substantially, and in this preliminary stage the aim has been to develop a simple model. In any case, it is considered that the differences are not very significant.

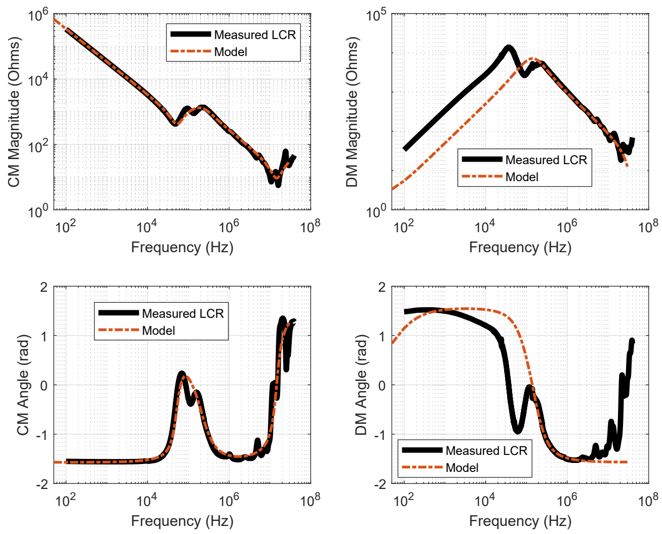

Fig. 3. CM and DM impedances of the PMSM. Measured Vs Estimated by the model

B. High Frequency Model for the Power Cable

The power cable is modelled using an universal PI type segmented circuit [15]. In order to improve the accuracy of the model, 20 segments are defined. It should be mentioned that only the CM model is considered, and the DM of the cable is not included, leading to more simplified equivalent circuit with less concentrated parameters. This is because in this work only the CM voltage and currents are going to be studied, so that the presented circuit is enough for that purpose.

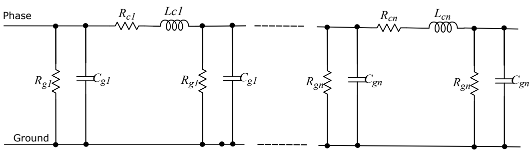

Fig. 4. Single phase high frequency PI type model for the power cable

The CM impedance of the cable is measured in the range of 100 Hz - 30 MHz using the LCR meter, model 11050-30M of CHROMA.

Using the experimentally measured impedances the values of the parameters of the equivalent circuit are calculated (see Table II). In the Fig. 5, the obtained curves with the proposed model for the amplitude and the angle of the CM impedance are compared with the curves measured experimentally. Even though the model overestimates slightly the resonances that appear in the amplitude curve, a fairly good agreement between experimental and modelled impedances can be appreciated.

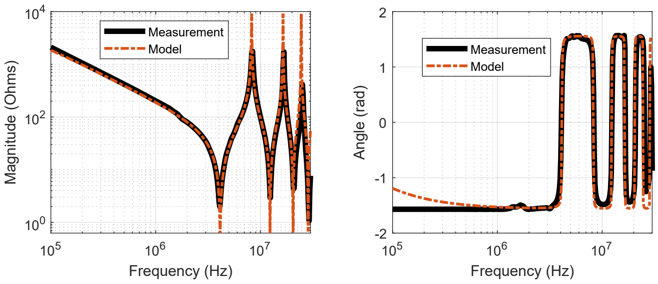

Fig. 5. CM impedance of the power cable. Measured Vs Estimated by the model

TABLE II
CALCULATED VALUES PER SEGMENT FOR THE PARAMETERS OF THE ELECTRICAL EQUIVALENT PI TYPE CIRCUIT

Parameter	Value	Parameter	Value
R_g	600 KΩ	R_c	0,015 Ω
C_g	6,67 pF	C_c	690 nF

C. *High Frequency Model for the PMSM & Power Cable System*

Once the PMSM model and the cable model are adjusted, in this section the complete motor-cable system behaviour is analysed. On one hand, the CM impedance of the cable-motor system is measured in the range between 100 Hz and 30 MHz using the LCR meter, model 11050-30M of CHROMA. On the other hand, the amplitude and the angle curves for the CM impedance are obtained coupling the previously tuned high frequency PMSM and cable models. The results are shown in the Fig. 6. The main resonances of the system are properly represented. However, there are some minor oscillations around the resonance situated about 2.5 MHz which are not very accurately modelled. Nevertheless, it is considered that the obtained precision is quite acceptable.

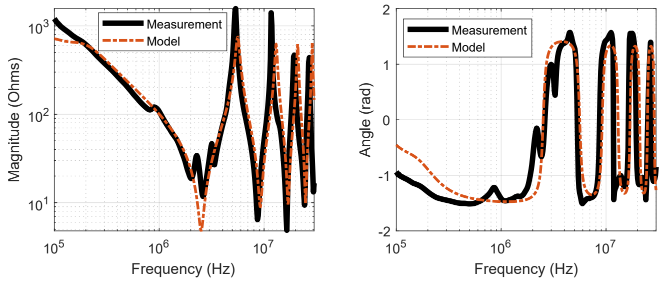

Fig. 6. CM impedance of the cable-motor system. Measured Vs Estimated by the models

III. High Frequency Simulations

In this section the operation behaviour of the overall electric drive system, comprising the motor, the cable and the inverter, is analysed from the perspective of the EMC. The simulations are carried out using the commercial system simulator software MATLAB-SIMULINK. The high frequency models described in the previous chapter are used for modelling the PMSM and the cables, whereas the inverter is modelled using the models provided by the SimScape library of MATLAB-SIMULINK. An advanced model is chosen for the IGBT's, which is explained in the next section.

A. *Description of the IGBT model*

The spectrum of the CM voltage generated by the inverter depends on the rising time of the voltage waveform. As it can be appreciated in the Fig. 7 and in the Fig. 8, the shorter the rising time is the wider the bandwidth of the spectrum is.

This rising time depends mainly on several parasitic parameters of the IGBT such as the gate resistance R_g, the collector-emitter capacitance C_{ce}, the collector-gate capacitance C_{cg} and the gate-emitter capacitance C_{ge}. Thus, in order to represent accurately the behaviour of the IGBT this parasitic parameters must be considered in the model. In the Fig. 7 the chosen model of the IGBT is described.

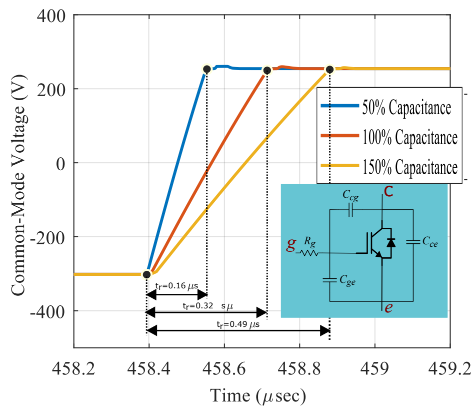

Fig. 7. CM voltage rising depending on the value of the parasitic capacitances. Changing C_{cg}, C_{ge}, C_{ce} in the same percentage

The values of the parasitic capacitances are not constant, but they depend on the collector-emitter V_{ce} voltage. Hence,

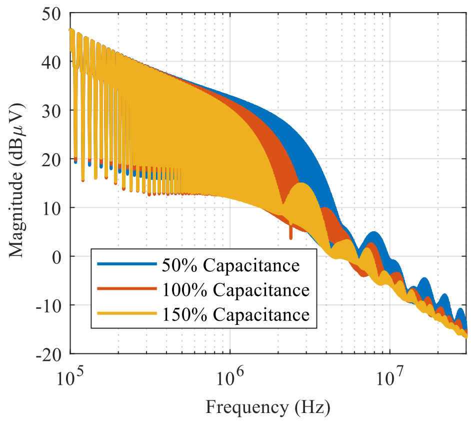

Fig. 8. Simulation result of the CM voltage Spectrum obtained for different parasitic capacitance values

these capacitances are defined by means of some characteristics curves obtained from the datasheet. Concerning the R_g resistance, it is considered constant and the value is obtained from the datasheet as well ($R_g = 2.5\Omega$).

In the Fig. 9 the rising of the CM voltage is shown. The result obtained with the model is compared with the signal measured experimentally at the output of the inverter. The slope of the modelled signal is constant during all the rising time so that it is a trapezoidal waveform. However, in the case of the real signal, more likely s-shape waveform, the slope is variable. This difference is due to several assumptions that are made in the implemented IGBT model. Nevertheless, it must be underlined that the bandwidth of the spectrum depends on the maximum slope value. The maximum slope of the real signal is very similar to the slope of the modelled signal, so that it is expected that the modelled spectrum is going to be very similar to the measured one. This point is checked in the next chapter (see the Fig. 16).

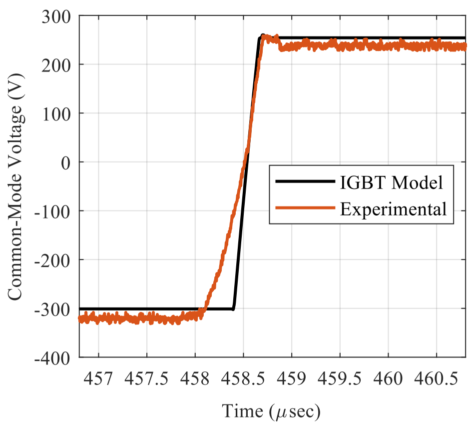

Fig. 9. Rising of the CM voltage at the output of the inverter. Measured Vs modelled

B. Simulation Results

In this section the results obtained in simulation are analysed. The simulations are carried out considering the complete electric drive system, as it is shown in the Fig. 10. The CM voltages are measured in both sides of the power converter, in the inverter side and in the motor side. In addition, the CM current is measured in the motor side ground connection.

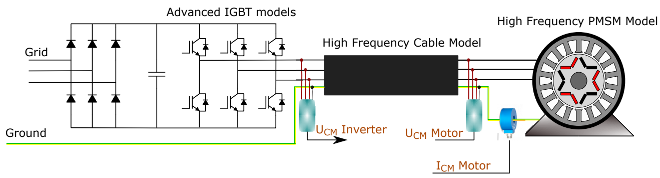

Fig. 10. Diagram of the simulated electric drive

In the Fig. 11 the CM voltage rising is plotted. The resonance caused by the cables creates an overvoltage at motor terminals. The overshooting amplitude and the oscillation frequency depend on the parameters of the power cable. Thus, they could vary significantly modifying the length of the cable.

The spectrums of both CM voltages, inverter side and motor side, along with the motor CM current are shown in the Fig. 11. In this graphic as well, the effect of the cable is clearly represented with the resonance that appears around 2.5 MHz. In addition, the attenuation at highest frequencies is accentuated by the effect of the cable, as the amplitude of the CM voltage spectrum decreases with a higher slope in the motor side. Concerning the CM current, the main resonance due to the cables can be appreciated as well.

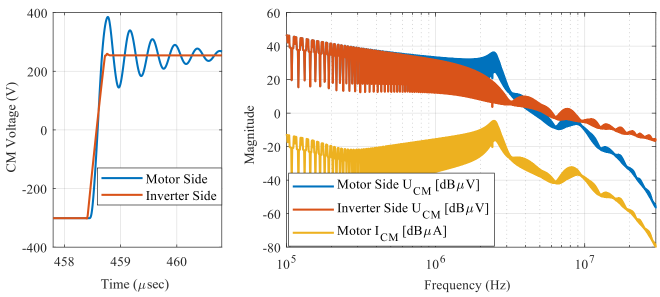

Fig. 11. CM voltage and current spectrums obtained in simulation

IV. Experimental Validation

In this section the proposed simulation model is validated by means of experimental test performed over an industrial electric drive. It consists of a Control Techniques Servo Driver, model M701-06420350A, and a 4.5 kW industrial PMSM. The CM current is measured using the transducer TEKBOX TCP1-150, combined with the attenuator TEKBOX TBFL1 (attenuation of 10 dB with a bandwidth of 9 kHz - 600 MHz). The CM voltages are measured using the probe TESTEC TT-SI9110 (bandwidth of 100 MHz). All signals are recorded in a YOKOGAWA oscilloscope, model DLM2024. The input impedance of the oscilloscope is set to 50 Ohms. In order to obtain enough resolution in the overall frequency bandwidth, 6.25 Msamples/s are stored during a single electric period of 20 milliseconds, with a sampling frequency of 312.5 MHz. The validation process is addressed in three different stages. First the motor model alone, second the motor-cable system, and finally the complete inverter-cable-motor system is validated. In the next sections these three stages are described.

Fig. 12. Experimental set-up

A. *Validation of the PMSM Model*

In order to validate the motor model, during the test the CM voltage waveforms are measured at motor terminals. Then the simulation is performed supplying the motor model with the experimentally measured CM voltage waveforms.

In the Fig. 13 the spectrum of the CM current is shown. There is a very good agreement between the simulation and the experimental results almost in the overall frequency range, except in the bandwidth of frequencies above 10 MHz. This is due to the induced noise in the voltage probes as it is explained in the next section (see Fig. 14)

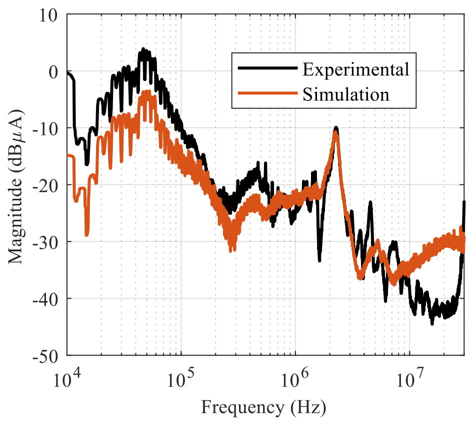

Fig. 13. Spectrum of the CM mode current. Motor model supplied in simulation by experimentally measured CM voltage waveforms at motor terminals

B. *Validation of the Cable-PMSM System Model*

In the second stage the cable-motor system is validated. The simulation is performed supplying the cable-motor system with experimentally measured CM voltages at the inverter output.

In the Fig. 14 the spectrum of the CM voltage at motor terminals is shown. It can be appreciated that the main resonance situated around 2.5 MHz is accurately represented by the model. Nevertheless, there is a slight difference in the bandwidth 4-8 MHz. The error in the bandwidth 10-30 MHz is not considered because in this frequency range the experimental measurement is not valid due to the voltage probe noise. In the Fig. 15 the spectrum of the CM current in the motor is plotted. The result is similar to the CM voltage, as the main resonance is accurately modelled, but there is a slight difference in the frequency range of 4-8 MHz. The CM voltage and the CM current, both are a little bit underestimated by the simulation model in the range of 4-8 MHz. However, the differences are not very high so that the simulation results could be considered reasonably accurate.

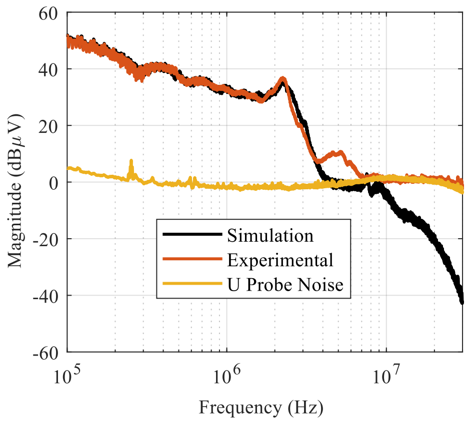

Fig. 14. Spectrum of the CM voltage at motor terminals. Cable-Motor model supplied in simulation by experimentally measured CM voltage waveforms at the output of the inverter

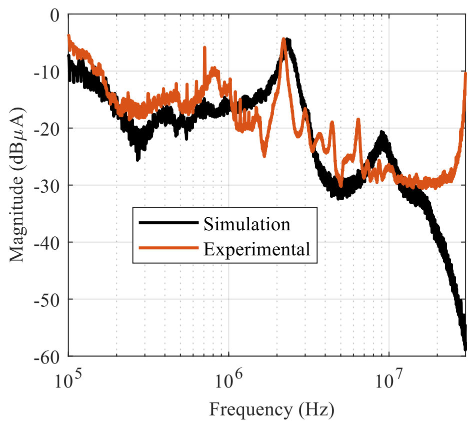

Fig. 15. Spectrum of the CM current in the motor. Cable-Motor model supplied in simulation by experimentally measured CM voltage waveforms at the output of the inverter

C. *Validation of the Overall Drive System Model*

Finally, the total drive system simulation is validated, performing the simulation described in the Fig. 10. In the

Fig. 16 the spectrum of the CM voltage generated by the inverter is shown. In general, the shapes of the simulated and the experimentally measured spectrums are to some extent similar, although there are some small differences in certain frequency margins. At the beginning the spectrum amplitude decreases 20 dB/Dec, up to 2 MHz, and then the slope changes to 40 dB/Dec. As it is well known, the frequency at which the slope changes, depends on the rising time of the CM voltage generated by the inverter.

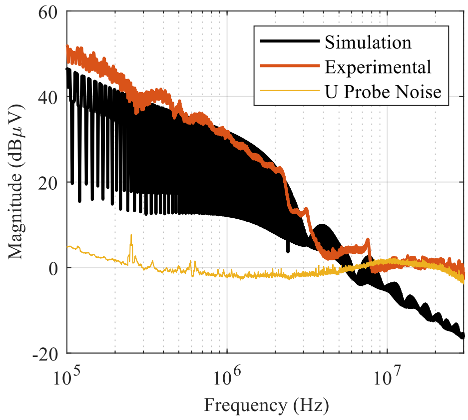

Fig. 16. Spectrum of the CM voltage at the output of the inverter. Simulation of the overall electric drive system

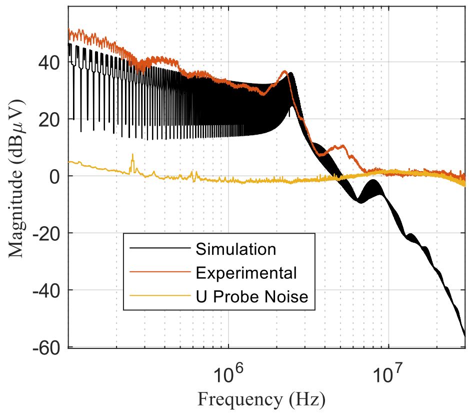

Fig. 17. Spectrum of the CM voltage at the motor terminals. Simulation of the overall electric drive system

Perhaps, this slope change is better appreciated in the spectrum of the CM voltage at motor terminals, which is plotted in the Fig. 17. In this case as well, the simulation results agree with the experimental measurements. It can be clearly seen the resonance created by the cables at 2.5 MHz, which is well estimated by simulation.

Finally, in the Fig. 18 the CM current in the motor is shown. It is slightly overestimated by simulations in the frequency range of 600 kHz - 2 MHz although the differences are not very significant. These differences could be due to the fact that the inverter output voltage is also somehow overestimated by simulations in this frequency range. In addition, there are some small amplitude oscillations in the spectrum obtained experimentally which are not reproduced by simulations. This could be due to many parasitic effects that are not reproduced by the cable and motor models. Probably, improving the models, these small oscillations could be also reproduced. But it could lead to more complex and more time-consuming calculations, and it is important to find a trade-off between accuracy and time consumption.

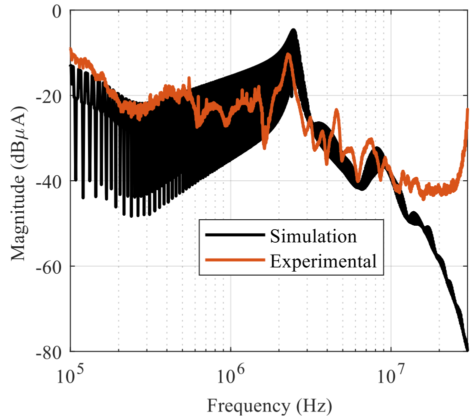

Fig. 18. Spectrum of the CM current in the motor. Simulation of the overall electric drive system

In general, a very good agreement can be observed between the simulation results and the experimental measurements at frequencies below 10 MHz. However, it can be appreciated that the differences are quite relevant at frequencies above 10 MHz, as aforementioned, due to the voltage probe noise. As future prospect, the measurement procedure and instruments should be improved in order to measure the CM current and voltages accurately in the total range of interest, 150 kHz - 30 MHz so as to validate the simulations in the overall frequency bandwidth.

V. Conclusions

In this paper a time-step simulation for the EMC analysis of PMSM electric drives is presented. By using this simulation, it is possible to analyse rather accurately, with a short computation time, the EMC compliance of the electric drives, considering the inverter, the power cable and the electrical motor.

The presented simulations are validated by some experiments performed over an industrial electric drive, as a reasonably good agreement between the simulation results and the experimental measurements are achieved.

The EMC compliance of electric devices must be evaluated in the frequency range of 150 kHz - 30 MHz. In spite of that, in this paper the behaviour of the electric drive is experimentally analysed at frequencies below 10 MHz, due to the electromagnetic noise induced in the voltage probes and current transducers. As future lines, more immune probes and transduces should be employed in order to avoid the effect of this electromagnetic noise. This way the simulations could be evaluated in the overall range of EMC frequencies.

REFERENCES

[1] S. Takahashi, S. Ogasawara, M. Takemoto, K. Orikawa, and M. Tamate, "Common-mode voltage attenuation of an active common-mode filter in a motor drive system fed by a PWM inverter," *IEEE Transactions on Industry Applications*, vol. 55, no. 3, pp. 2721–2730, 2019.

[2] C. T. Morris, D. Han, and B. Sarlioglu, "Reduction of Common Mode Voltage and Conducted EMI Through Three-Phase Inverter Topology," *IEEE Transactions on Power Electronics*, vol. 32, no. 3, pp. 1720–1724, 2017.

[3] Z. Shen, D. Jiang, T. Zou, and R. Qu, "Dual-Segment Three-phase PMSM with Dual Inverters for Leakage Current and Common-mode EMI Reduction," *IEEE Transactions on Power Electronics*, vol. PP, no. c, pp. 1–1, 2018. [Online]. Available: https://ieeexplore.ieee.org/document/8440757/

[4] B. Revol, J. Roudet, J. L. Schanen, and P. Loizelet, "EMI study of three-phase inverter-fed motor drives," *IEEE Transactions on Industry Applications*, 2011.

[5] A. F. Moreira, T. A. Lipo, G. Venkataramanan, and S. Bernet, "High-frequency modeling for cable and induction motor overvoltage studies in long cable drives," *IEEE Transactions on Industry Applications*, vol. 38, no. 5, pp. 1297–1306, 2002.

[6] A. Boglietti and E. Carpaneto, "An Accurate Induction Motor High-Frequency Model for Electromagnetic Compatibility Analysis," *Electric Power Components and Systems*, 2001.

[7] M. S. Toulabi, L. Wang, L. Bieber, S. Filizadeh, and J. Jatskevich, "A Universal High-Frequency Induction Machine Model and Characterization Method for Arbitrary Stator Winding Connections," *IEEE Transactions on Energy Conversion*, vol. PP, no. c, p. 1, 2019.

[8] C. Bi, K. Jia, Y. Wu, L. Dong, H. Li, W. Yao, G. Liu, and H. Zhang, "High-frequency electric-motor modelling for conducted CM current prediction in adjustable speed drive system," 2018. [Online]. Available: www.ietdl.org

[9] X. Lu, S. Zhang, C. Liu, P. Xie, and H. Chen, "Modeling of common-mode current in motor cable of inverter-fed motor drive system," in *2016 Asia-Pacific International Symposium on Electromagnetic Compatibility, APEMC 2016*, 2016.

[10] H. Miloudi, A. Bendaoud, M. Miloudi, S. Dickmann, and S. Schenke, "Common mode and differential mode characteristics of AC motor for EMC analysis," *IEEE International Symposium on Electromagnetic Compatibility*, vol. 2016-Novem, pp. 765–769, 2016.

[11] G. Vidmar and D. Miljavec, "A Universal High-Frequency Three-Phase Electric-Motor Model Suitable for the Delta- and Star-Winding Connections," *IEEE Transactions on Power Electronics*, vol. 30, no. 8, pp. 4365–4376, 2015.

[12] M. Mohammadi-Rostam, M. Shahabi, and A. A. Shayegani-Akmal, "High frequency lumped parameter model for EMI problems and over voltage analysis of Induction motor," *Journal of Electrical Engineering*, vol. 13, no. 3, pp. 278–283, 2013.

[13] C. Purcarea and P. Mutschler, "Investigation of EMI reduction techniques using time domain simulation of drives," in *IECON Proceedings (Industrial Electronics Conference)*, 2009.

[14] B. Mirafzal, G. L. Skibinski, and R. M. Tallam, "Determination of Parameters in the Universal Induction Motor Model," *IEEE Transactions on Industry Applications*, vol. 45, no. 1, 2009.

[15] M. A. Gries and B. Mirafzal, "Permanent magnet motor-drive frequency response characterization for transient phenomena and conducted EMI analysis," in *Conference Proceedings - IEEE Applied Power Electronics Conference and Exposition - APEC*, 2008.

[16] J. Sun and L. Xing, "Parameterization of three-phase electric machine models for EMI simulation," *IEEE Transactions on Power Electronics*, vol. 29, no. 1, pp. 36–41, 2014.

[17] B. Mirafzal, G. L. Skibinski, R. M. Tallam, D. W. Schlegel, and R. A. Lukaszewski, "Universal induction motor model with low-to-high frequency-response characteristics," *IEEE Transactions on Industry Applications*, vol. 43, no. 5, pp. 1233–1246, 2007.

BIOGRAPHIES

Gaizka Almandoz was born in Arantza, Spain. He received the B.Sc. and Ph.D. degrees in electrical engineering from Mondragon Unibertsitatea, Mondragon, Spain, in 2003 and 2008, respectively. Since 2003, he has been with the Electronics and Computing Department, Faculty of Engineering, Mondragon Unibertsitatea, where he is currently an Associate Professor. His current research interest includes electrical machine design, modeling, and control.

Sergio Zarate was born in Vitoria-Gasteiz, Spain. He received the B.Sc., M.Sc. and Ph.D. degrees in electrical engineering at Mondragon Unibertsitatea, Mondragon, Spain, in 2012, 2014 and 2018, respectively. Since 2018, he has been with the Electronics department of the Faculty of Engineering of Mondragon Unibertsitatea, where he is currently a Lecturer and Researcher. His current research interests include drives, electrical machines vibration and permanent magnet machine design and optimization

Aritz Egea received the degree in electrical engineering from the University of Mondragon, Mondragon, Spain, in 2009 and the Ph.D. degree in electrical engineering in 2012. Currently he is an Associated Professor in the Faculty of Engineering, Mondragon Unibertsitatea. His current research interests include electrical machine design and control and electromagnetic actuators.

Yerai Moreno was born in Irún, Spain, in October 1996. He received the Bachelor Degree in Electrical Engineering from University of the Basque Country, Donostia- San Sebastián, Spain, in 2018. Since 2018, he has been researching with the Department of Electrical Machines, Faculty of Engineering, Mondragon Unibertsitatea, where he is currently working toward the Ph.D. degree.

Ander Urdangarin was born in Ordizia. Spain, in February 1982. He received the B.S degree in Automatic and industrial electronics from Mondragon Unibertsitatea, Mondragón, Spain in 2009. Between 2010 - 2012, he was with the Department of Electronics, Faculty of Engineering of Mondragon Unibertsitatea. Since 2012 he is member of ORONA. His current research interests include power electronics design, modeling, and control.

Roberto Moreno was born in Eibar, Spain, in May 1974. He received the B.S. degree in electronic engineering from Mondragon Unibertsitatea, Mondragón, Spain, in 1998. Since 1998, he has been with the Department of Electronics (now Hardware Systems and Comunications Área), in Ikerlan Research Center. Since 2008 he is head of EMC and non functional requirements laboratory and researcher. His current research interests include electrical and electronic behaviour analisys and simulation of power and control electronics in the EMC area.